Recent Changes in Southern Ocean Circulation and Climate

Brady S Ferster, Bulusu Subrahmanyam, Anthony Arguez

Recent Changes in Southern Ocean Circulation and Climate

Brady S. Ferster, Bulusu Subrahmanyam, and Anthony Arguez

***Abstract*— The Southern Ocean (SO) is essential to global ocean circulation and climate variability. The strength and position of the Southern Hemisphere (SH) westerlies are largely thought to be driving recent trends in the SO. We find increasing SH wind speeds between 45° S and 60° S by 0.0075 ± 0.00013 m·s^{-1}·year^{-1} and decreasing in the mid-latitude region of -0.0054 ± 0.00011 m·s^{-1}·year^{-1}. Mean surface temperatures (depth-integrated ocean heat content) are significantly increasing at 0.0066 ± 0.0057 °C·year^{-1} (3.8 ± 2.4 W·m^{-2}), although significantly decreasing within the high-latitude Pacific and Atlantic basins. Sea level change indicates that the median trend in the SH is 3.1 ± 0.69 mm·year^{-1}, although there is a negative trend in the central South Pacific. Our analysis concludes that changes in surface wind speeds are significantly driving regional changes in sea level, heat content, and surface temperatures in the SH high latitudes, contributing to negative trends in the South Pacific.**

***Index Terms*— Ocean heat content (OHC), sea surface height (SSH), sea surface temperature (SST), Southern Ocean (SO), winds.**

I. Introduction

THE Southern Ocean (SO) plays a pivotal role in the global-scale meridional overturning circulation, as it distributes mass, heat, and freshwater between the Atlantic, Pacific, and Indian Oceans [1]. The strong Southern Hemisphere (SH) westerlies force the eastward-flowing Antarctic Circumpolar Current (ACC) and drive Ekman upwelling, essential components in global circulation. The westerlies are known to exhibit large natural variability, oscillating on weekly to centennial timescales [2], [3]. Recent studies have found that the westerlies have shifted southward, largely driven by the Antarctic ozone hole [3], [4], and are thought to be a major influence on the recent restructuring of ACC fronts [5], [6], which could have major implications on circulation, surface mixing, and climate variability.

The SO is of global significance, regulating and transporting heat, nutrients, and gases throughout the oceans. Significant warming and freshening have been observed within the SO [7], [8]. Similar to the westerlies [3], [4], recent changes in the SO temperature and salinity are driven through greenhouse gas emissions and ozone depletion [7]. Further significant changes in ocean heat content (OHC) [9], sea level [10], and sea ice extent [11] have all been observed through satellite and *in situ*-based data analyses. As a result, regional-scale changes in wind, salinity, and temperature influence thermodynamic and dynamic forcing, such as sea ice formation and surface mixing.

Historically, *in situ* observations have been sparse in the SO [12]. Satellite products such as surface winds, sea level, and sea surface temperature (SST) provide high-quality data with improved spatial resolution that extends back through the 1990s. For this analysis, the long timescales of the products are ideal to investigate the SO trends and variability. An investigation into the surface winds, sea level anomalies (SLAs), SST, and OHC allows for an in-depth examination of the current state of the SO climate and circulation. Expected results are increased SST in the mid-latitude SO and decreased SST in the high-latitude SO, with similar spatial results in OHC. We further hypothesize increased magnitude of surface winds and SLA.

II. Data and Methodology

A. Satellite Observations

We have used the daily NOAA's blended sea winds product in this letter (research quality version 1.2). The blended product contains wind vector velocities with daily 0.25° resolution from July 1987 to 2017, utilizing merged satellite-derived wind measurements from multiple missions for global coverage. The daily products were binned and averaged for monthly timescales in this analysis. Further description on the data can be found through [13] and [14].

Sea surface height (SSH) data are available by the Copernicus Marine Environment Monitoring Service in near real time, as are reprocessed products that allow for quality control checks and cross-calibration processes to remove residual orbit error. The multimission gridded SLA and anomalous currents are in reference to the 20-year mean of SSH (1993–2012). Both reprocessed and near real-time SLA products are used in this analysis are from January 1993 to December 2017 in 0.25° spatial resolution.

Liquid water equivalent thickness anomalies (LWE) are estimated using the twin satellites Gravity Recovery and Climate Experiment (GRACE) [15]. This mission measures regional mass changes of the earth's land water storage, ocean, and ice content. In this analysis, GRACE LWE is analyzed from 2002 to 2017 in the monthly format with 1° resolution [15]. Information regarding the estimation and validation of GRACE monthly mass release 5.0 refer to [16] and [17]. Methods of [18] and [19] are used to estimate OHC anomalies from sea level and LWE anomalies. Jayne *et al.* [19] indicate that

Manuscript received June 27, 2018; revised September 5, 2018, October 11, 2018, and October 23, 2018; accepted November 7, 2018. The work of B. S. Ferster was supported by the NASA/South Carolina Space Grant Graduate Assistantship. *(Corresponding author: Brady S. Ferster.)*

B. S. Ferster and B. Subrahmanyam are with the School of the Earth, Ocean, and Environment, University of South Carolina, Columbia, SC 29208 USA (e-mail: bferster@seoe.sc.edu).

A. Arguez is with the National Oceanographic and Atmospheric Administration, National Centers for Environmental Information, Asheville, NC 28801 USA.

Color versions of one or more of the figures in this letter are available online at http://ieeexplore.ieee.org.

Digital Object Identifier 10.1109/LGRS.2018.2880589

the OHC anomalies are throughout the entire depth-integrated column; however, Lyman and Johnson [12] indicate that the strong correlation of SLA to OHC anomalies is primarily within the 300–1800 m depths.

SST data from a Group for High Resolution Sea Surface Temperature (GHRSST) version 2.0 [20] can be downloaded globally from September 1991 to 2016 [21]. This level 4 product combines infrared and microwave satellite-derived data with *in situ* observations to produce a high-resolution product. For this analysis, the 0.2° resolution GHRSST data product was used for full years (1992–2016) to prevent seasonal bias, and we have removed all data points with satellite-derived fractional sea ice in the high latitudes.

B. Methods for Anomalies and Statistical Tests

To estimate the anomalies of surface winds, sea level, and SST, the 20-year monthly climatological means (1993–2012) have been removed, the same time period to that of the processed SLA product. Removing the same 20-year period of climatology preserves the conclusions of the analyses through standardizing the anomalies. OHC anomalies use the mean of 2005 to 2012 based on the years of available LWE data. To estimate trends, a robust regression of the yearly averaged anomalies is used to better account for outliers and autocorrelation through a bisquare method. Statistics are tested under the assumption of being zero and are considered significant (nonzero) using an alpha of 0.05. Trends are presented within the 95% confidence interval. In each instance, grid cells with sea ice are treated as missing values and are ignored. The trends are presented in the unit year^{-1}. The ACC region is defined as 45° S–60° S, the mid-latitude area is 30° S–45° S, and the high latitudes are poleward of 60° S.

III. Results and Discussion

A. Surface Winds

Fig. 1 illustrates the increasing wind speeds in the ACC region and decreasing magnitude in the mid-latitude regions; the trends contoured in black are significantly different from zero. The 1988–2017 significant trends indicate rates between -0.060 and 0.053 m·s^{-1}·year^{-1}. The SH mean trend is 0.00057 ± 0.00017 m·s^{-1}·year^{-1} (median of 0.0031 m·s^{-1}·year^{-1}) and a standard deviation of 0.041 m·s^{-1}·year^{-1}. The trends are significant throughout much of the ACC and the mid-latitude Indian basin. Moreover, there are significant positive trends along the eastern boundary of each ocean basin (mid-latitudes), a negative trend within the Indian basin western boundary and throughout each of the mid-latitude central basins. The mean trend in the mid-latitudes is -0.0054 ± 0.00011 m·s^{-1}·year^{-1} and is 0.0075 ± 0.00013 m·s^{-1}·year^{-1} in the ACC region.

The SH westerlies have intensified and shifted poleward in recent decades [3], [4]. In the most recent period of 2010–2017, surface wind anomalies have considerably increased within the ACC region of the Atlantic and Indian basins and decreased within the central South Pacific and Indian Oceans. There are large anomalies found along the Drake Passage, New Zealand, and the western South American and South African coasts. The large positive anomalies within the ACC region of the Indian and Atlantic basins during 2010–2017 support the strong positive trends of the region and intensification of surface wind speeds. Negative wind speed trends are indicated within the mid-latitude Pacific, Indian, and Atlantic basins from 1988 to 2017.

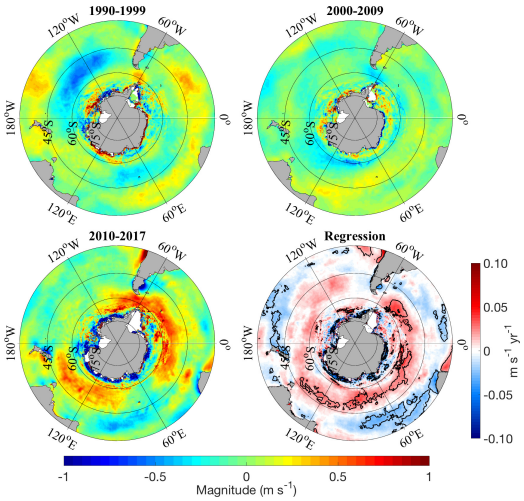

Fig. 1. Decadal means and trends of the surface wind speed anomalies from 1988 to 2017. Trends significant at the 95% confidence level are contoured in black.

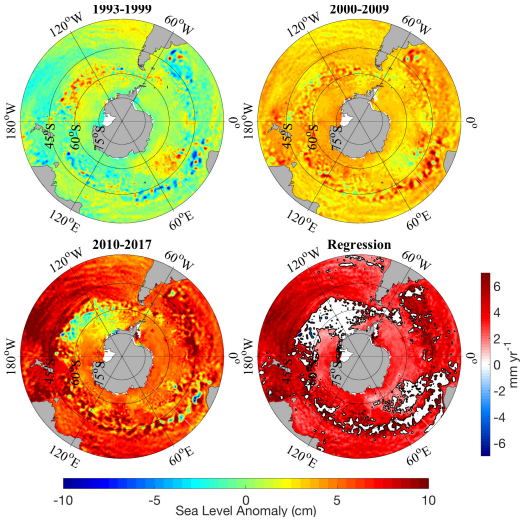

Fig. 2. Decadal means and trends of SLAs from 1993 to 2017. Trends significant at the 95% confidence level are contoured in black.

B. Sea Level Anomalies

Fig. 2 depicts the mean decadal SLA and trends, with significant trends contoured in black. Similar to surface winds, the largest anomalies occur between 2010 and 2017. Within this period, the mean (median) SLA is 5.8 cm (5.7 cm). Regions like the mid-latitude western Pacific and Atlantic basins indicate that the mean 2010–2017 anomalies are 8.4 and 6.7 cm, respectively. These regions demonstrate the largest trends and wind speed anomalies within the 2010–2017 period. In the South Indian, Atlantic, and Pacific Oceans, the western boundaries are significantly increasing in sea level, while significantly decreasing in the central South Pacific (160° W–120° W, 50° S–60° S) and Atlantic–Indian exchange.

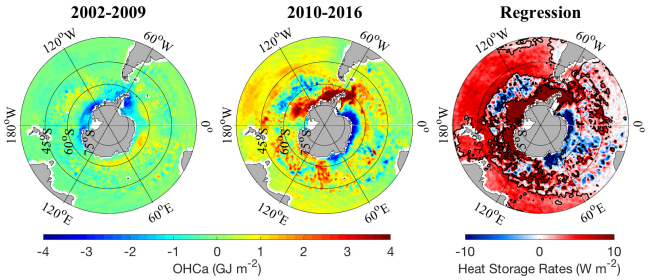

Fig. 3. Decadal mean OHC anomalies and trends of ocean heat storage rates from 2002 to 2016. Trends significant at the 95% confidence level are contoured in black.

These SLA trends further show the intensification of the SH sea level rise. Much of the SH reveals statistically significant trends, the mean (median) of 3.1 ± 0.69 mm·year^{-1} (3.0 mm·year^{-1}) and a standard deviation of 1.8 mm·year^{-1}. Regions such as the central and western South Pacific, Indian, and Atlantic Oceans suggest that significant trends can be larger than 6.0 mm·year^{-1}, posing as large outliers from the mean positive trend of 3.3 ± 0.61 mm·year^{-1} and a standard deviation of 1.4 mm·year^{-1}. Despite such large positive trends, the South Pacific, Drake Passage, and within the Agulhas retroflection all indicate significant negative trends of -1.6 ± 0.47 mm·year^{-1} and a standard deviation of 1.4 mm·year^{-1}.

Past studies estimate the global rate of sea level change to be 3.2 ± 0.4 mm·year^{-1} via satellite altimetry and 2.8 ± 0.8 mm·year^{-1} through observational measurements during 1993 to 2009 [22]. Between 2003 and 2011, the rate of sea level change slowed to 2.4 mm·year^{-1} [23], but could be largely influenced by land-driven hydrology and water storage [24]. The mean rate of sea level change for the SO in this analysis is 3.1 ± 0.69 mm·year^{-1} and a standard deviation of 1.8 mm·year^{-1} from 1993 to 2017, which is larger than previous global mean rates. However, as shown in Fig. 2, there are rates in the SH between –9.6 and 12.2 mm·year^{-1}. Moreover, the 2010–2017 anomalies indicate the large magnitude of anomalies compared to the 2000–2009 period. These results indicate the recent large magnitude of SLAs and the broad-scale positive trends in sea level change between 1993 and 2017.

C. Ocean Heat Content Anomalies

Fig. 3 shows that OHC anomalies have largely increased between 2010 and 2016, similar to wind and SLAs. There are strong positive anomalies in the mid-latitude Pacific and western Indian Ocean basins and near the Drake Passage. The 15-year trends illustrate that much of the South Pacific and Indian Oceans and the central South Atlantic Ocean have significant positive trends. The mean (median) positive trend is 6.1 ± 3.3 (4.4) W·m^{-2}. Significant negative trends occur within the ACC region of the Pacific basin and the Atlantic–Indian basin exchange. The mean (median) negative trend is -4.7 ± 2.2 (-3.3) W·m^{-2}. The mean (median) trend in the entire SO is 3.8 ± 2.4 (3.5) W·m^{-2} and a standard deviation of 7.5 W·m^{-2}.

Chambers and Bonin [16] concluded that SSH data in the SO are strongly correlated with OHC anomalies between 300 and 1800 m depth. Results for OHC anomalies and

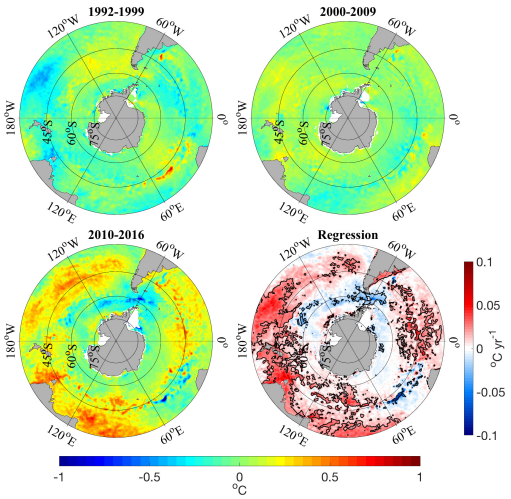

Fig. 4. Decadal mean SST anomalies and trends from 1991 to 2016. Trends significant at the 95% confidence level are contoured in black.

trends in this analysis are spatially similar to that of SLA, despite including the ocean mass data in estimating OHC. The similarities with SLA stress the importance of OHC within the SO. A difference between OHC and SLA trends is along the Antarctic coast (0° –60° E). OHC trends indicate negative heat storage values but are collocated in a region of increasing SLA. This could be a result of different temporal mean periods, salinity, or runoff.

The trends along the Antarctic coast are comparatively large. OHC anomalies derived from SLA and ocean mass allow for reduced errors in regions like the high-latitude SO [19]; however, poleward of the ACC is known to be dominated by salinity rather than temperature. Taking this into consideration, the results poleward of 60° S should be taken with caution and examined with the use of salinity. Willis *et al.* [9] have shown global OHC to be steadily increasing between 1993 and 2003, increasing globally 0.86 W·m^{-2} during that time. The SO is known to experience the greatest global ocean warming from 1960 to 2015, with large changes in OHC to depths of 2000 m [25]. Their results suggest that the SO contributes 30% (28%) of the global OHC increase from 0 to 2000 m (0–700 m) between 1998 and 2015. Cheng *et al.* [25] concluded that the SO plays a major role in global heat storage through the overturning circulation, increasing $\sim 4.26 \times 10^{22}$ J between 1998 and 2015 in the SO along.

D. Sea Surface Temperature Anomalies

The 2010–2016 period indicates the large-scale warming throughout the mid-latitude SO. The 2010–2016 mean anomalies are largely positive during this period, indicative of the temporal trend throughout the mid-latitude regions. The 2010–2016 mean anomaly is 0.083 °C, larger than either of the other periods, indicative of a clear warming pattern and increased magnitude of anomalies in the 2010–2016 period. The mean SST trend is 0.0066 ± 0.0057 °C·year^{-1} and a standard deviation of 0.015 °C·year^{-1} in the SO, as shown in Fig. 4. The large variability in the trends is a result of latitudinal differences. Decadal analyses of SH SSTs show positive trends in much of the mid-latitude and ACC

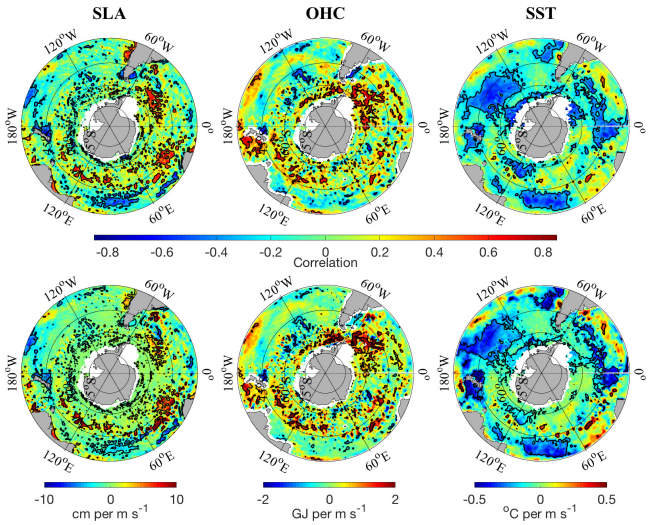

Fig. 5. Pearson's correlation coefficients and robust regressions between surface wind speed anomalies and SLA, OHC, and SST anomalies. The comparisons of SLA are between 1993 and 2017, OHC between 2002 and 2016, and SST from 1992 to 2016. Positive (red) values indicate a positive relationship between surface wind anomalies and the variables. Significant statistics at the 95% confidence level are contoured in black.

region and negative in the South Pacific basin (50° S–60° S), the Drake Passage, and Agulhas region. Trends are statistically significant throughout much of the SO. The South Pacific and Atlantic–Indian exchange show significantly negative trends, and the mid-latitudes are significantly positive. These results indicate significant cooling (negative) trends in SST in the high-latitude SO and warming (positive) trends within the SH subtropics and mid-latitudes. The largest trends of -0.10 ± 0.0094 °C·year^{-1} are within the Agulhas retroflection, but the mean negative trend is -0.016 ± 0.0048 °C·year^{-1} between the Drake Passage, central South Pacific, and the Atlantic–Indian exchange. The mean high-latitude trend indicates cooling (-0.0012 ± 0.0050 °C·year^{-1}), whereas the mid-latitudes indicate warming (0.014 ± 0.0056 °C·year^{-1}).

The mid-latitude regions of the western South Atlantic, Pacific, and Indian Oceans are increasing by 0.050 °C·year^{-1}, nearly four times greater than the mean mid-latitude trend of 0.014 ± 0.0056 °C·year^{-1}. Similar SST trends are discussed in [26] using Advanced Very High Resolution Radiometer data between 1982 and 2016. These results illustrate that there is significant warming in the mid-latitudes and cooling throughout much of the high-latitude SO.

E. Role of Surface Winds in the Southern Ocean Climate

Surface winds are the major driving force on ocean dynamics. Surface winds play a strong role in forcing ocean currents and work to induce ocean mixing. Within the SO, the strong winds drive water circulation and influence the vertical structure and distribution of heat, nutrients, and gases. In the SH, there are strong correlations and trends (Fig. 5) between SLA, OHC, and SST with surface wind anomalies.

SLAs are negatively correlated with surface wind speeds in the western South Pacific, the South Indian basin, and the Agulhas Current and positively correlated throughout much of the ACC and high-latitude Atlantic and Indian basins. The mean (maximum) significant negative correlation is -0.43 (-0.85) and positive is 0.44 (0.79). These correlations indicate the moderate-to-strong relationship between SLA and wind speeds. Positive trends along the Agulhas retroflection, the Malvinas, and the high-latitude Indian basin have slopes greater than 10 cm of SLA per 1 m·s^{-1} anomaly in wind speed, with maximum significant values in these regions of 25.2 cm per m·s^{-1}. The median positive significant value is 4.45 ± 1.91 cm per m·s^{-1}. The significant negative trends suggest slopes as large as -16.2 cm per m·s^{-1}, but a mean value of -3.24 ± 0.96 cm per m·s^{-1}. These results illustrate that surface wind speeds are significantly driving SLA in the high-latitude Atlantic and Indian basins, western South Pacific, and the South Indian Ocean.

Correlations between the SH wind and OHC anomalies indicate a significant positive relationship throughout much of the ACC and a negative relationship in the southeastern Indian Ocean and high-latitude South Pacific. The mean (maximum) significant negative correlation is -0.54 (-0.90) and positive is 0.55 (0.91), indicating the strong role of the surface wind speed on OHC. The correlations of OHC and SLA are similar to the high-latitude regions, suggesting that much of the SLA and OHC are positively driven by the surface winds in the Atlantic and Indian basins and driving negative OHC anomalies in the South Pacific basin. The mean (maximum) statistically significant high-latitude and ACC positive trend is 1.74 ± 0.47 (6.62) GJ per m·s^{-1} and negative trend is -1.34 ± 0.41 (-7.05) GJ per m·s^{-1}. These results show the broad-scale ocean warming in the South Atlantic and Indian basin high latitudes and cooling in the South Pacific basin as a result of wind speed anomalies.

Correlations with SST anomalies indicate a significant negative relationship throughout much of the South Pacific, Indian, and Atlantic Oceans, the Drake Passage, and the Malvinas region. The mean (maximum) significant negative correlation is -0.47 (-0.78) and positive is 0.42 (0.99). Positive relationships in the mid-latitude Western Indian and Atlantic basins are likely associated with wind-driven currents moving warm waters from the tropics to the mid-latitudes. Negative correlations in the high-latitude Pacific, South Atlantic, and Eastern Indian basin are driven by upwelling waters and surface currents and evaporative cooling, where increasing winds are associated with decreasing SST. The mean (maximum) significant positive trend is 0.47 ± 0.14 (1.76) °C per m·s^{-1} and negative trend is -0.26 ± 0.06 (-0.99) °C per m·s^{-1}. The slopes suggest broad-scale surface cooling in the South Pacific, Atlantic, and Indian basins and warming in the Malvinas and Agulhas regions as a result of positive changes in wind speed.

IV. Conclusion

The SO is a major driver in global circulation and offers insight into a deeper understanding of global-scale climate changes and variability. This analysis explores recent decadal changes in the SO winds, SLA, OHC, and SST. Analysis of the SH wind speeds illustrates the intensification of 0.0075 ± 0.00013 m·s^{-1}·year^{-1} throughout the ACC and much of the eastern ocean basins, while decreasing intensity in the mid-latitudes by -0.0054 ± 0.00011 m·s^{-1}·year^{-1}. The SH mid-latitudes are shown to be increasing in sea level,

SST, and OHC. The high latitudes and Antarctic coast are largely decreasing in heat content and sea level in the central South Pacific and Atlantic–Indian basin exchange, but show negative trends outside these regions. The mean SST (OHC) trend in the SO is 0.0066 ± 0.0057 °C year^{-1} (3.8 ± 2.4 W·m^{-2}). SST and OHC are increasing in the mid-latitude regions and decreasing within the Central Pacific and the Atlantic–Indian basin exchange. Trends in SLA indicate that the median SO sea level rise is 3.1 ± 0.69 mm·year^{-1}, with regions such as the western South Pacific and Atlantic greater than 6.0 mm·year^{-1}. Conversely, the central South Pacific, Drake Passage, and the Atlantic–Indian basin exchange are all regions of negative sea level trends.

Mean decadal anomalies suggest amplification of changes in surface winds, sea level, OHC, and SST during the 2010–2017 period. The recent anomalies display increased trends since the 2000–2009 period, further driving the 1993–2017 trends. Correlations and regressions further indicate that surface winds are significantly driving changes in the SO, driving increased SLA and OHC anomalies in the high-latitude Atlantic and Indian basins, while supporting decreased SLA, OHC, and SST in the high-latitude South Pacific Ocean. In conclusion, our results indicate the significance of surface wind speeds in driving large-scale changes in sea-level dynamics through ocean–atmosphere interactions.

Acknowledgment

NOAA's blended sea winds product (research quality version 1.2) can be accessed from ftp://eclipse.ncdc.noaa.gov/pub/seawinds/SI/uv/. Sea surface height data can be downloaded through Copernicus (http://marine.copernicus.eu/services–portfolio/access–to–products/) as product identifiers SEALEVEL_GLO_PHY_L4_NRT_OBSERVATIONS_008_046 (near real–time) and SEALEVEL_GLO_PHY_L4_REP_OBSERVATIONS_008_047 (reprocessed). GRACE ocean mass data (podaac–ftp.jpl.nasa.gov/allData/tellus/L3/ocean_mass/RL05/netcdf) and GHRSST data (podaac-ftp.jpl.nasa.gov/allData/ghrsst/data/GDS2/L4/GLOB/CMC/CMC0.2deg/v2) can be downloaded from JPL/PODAAC. The surface density values are from the 2005 to 2012 monthly mean World Ocean Atlas 2013 (https://www.nodc.noaa.gov/OC5/woa13/woa13data.html) and McDougall and Barker (2011) Gibbs Sea Water Oceanographic Toolbox of TEOS–10 (http://www.teos–10.org/pubs/gsw/html/gsw_contents.html) is used to estimate ocean heat content.

References

[1] J. Marshall and K. Speer, "Closure of the meridional overturning circulation through Southern Ocean upwelling," *Nature Geosci.*, vol. 5, no. 3, pp. 171–180, 2012, doi: 10.1038/ngeo1391.

[2] D. W. Thompson and J. M. Wallace, "Annular modes in the extratropical circulation. Part I: Month-to-month variability," *J. Climate*, vol. 13, no. 5, pp. 1000–1016, 2000, doi: 10.1175/1520-0442(2000)013<1000:AMITEC>2.0.CO;2.

[3] D. W. J. Thompson and S. Solomon, "Interpretation of recent southern hemisphere climate change," *Science*, vol. 296, no. 5569, pp. 895–899, 2002, doi: 10.1126/science.1069270.

[4] D. W. J. Thompson, S. Solomon, P. J. Kushner, M. H. England, K. M. Grise, and D. J. Karoly, "Signatures of the Antarctic ozone hole in Southern Hemisphere surface climate change," *Nature Geosci.*, vol. 4, pp. 741–749, Oct. 2011, doi: 10.1038/ngeo1296.

[5] S. Dong, J. Sprintall, and S. T. Gille, "Location of the Antarctic polar front from AMSR-E satellite sea surface temperature measurements," *J. Phys. Oceanogr.*, vol. 36, pp. 2075–2089, Nov. 2006, doi: 10.1175/JPO2973.1.

[6] S. M. Downes, A. S. Budnick, J. L. Sarmiento, and R. Farneti, "Impacts of wind stress on the Antarctic Circumpolar Current fronts and associated subduction," *Geophys. Res. Lett.*, vol. 38, no. 11, p. L11605, 2011, doi: 10.1029/2011GL047668.

[7] N. C. Swart, S. T. Gille, J. C. Fyfe, and N. P. Gillett, "Recent Southern Ocean warming and freshening driven by greenhouse gas emissions and ozone depletion," *Nature Geosci.*, vol. 11, pp. 836–841, Sep. 2018, doi: 10.1038/s41561-018-0226-1.

[8] P. J. Durack and S. E. Wijffels, "Fifty-year trends in global ocean salinities and their relationship to broad-scale warming," *J. Climate*, vol. 23, pp. 4342–4362, 2010, doi: 10.1175/2010JCLI3377.1.

[9] J. K. Willis, D. Roemmich, and B. Cornuelle, "Interannual variability in upper ocean heat content, temperature, and thermosteric expansion on global scales," *J. Geophys. Res. Oceans*, vol. 109, no. C12036, pp. 1–13, 2004, doi: 10.1029/2003JC002260.

[10] C. D. Rye *et al.*, "Rapid sea-level rise along the Antarctic margins in response to increased glacial discharge," *Nature Geosci.*, vol. 7, no. 10, pp. 732–735, 2014, doi: 10.1038/ngeo2230.

[11] R. Kwok, J. C. Comiso, T. Lee, and P. R. Holland, "Linked trends in the South Pacific sea ice edge and Southern Oscillation Index," *Geophys. Res. Lett.*, vol. 43, no. 19, pp. 10295–10302, 2016, 10.1002/2016GL070655.

[12] J. M. Lyman and G. C. Johnson, "Estimating global ocean heat content changes in the upper 1800 m since 1950 and the influence of climatology choice," *J. Climate*, vol. 27, no. 5, pp. 1945–1957, 2014, doi: 10.1175/JCLI-D-12-00752.1.

[13] G. Peng *et al.*, "Evaluation of various surface wind products with OceanSITES buoy measurements," *Weather Forecasting*, vol. 28, no. 6, pp. 1281–1303, 2013, doi: 10.1175/WAF-D-12-00086.1.

[14] H.-M. Zhang, J. J. Bates, and R. W. Reynolds, "Assessment of composite global sampling: Sea surface wind speed," *Geophys. Res. Lett.*, vol. 33, no. 17, p. L17714, 2006, doi: 10.1029/2006GL027086.

[15] D. P. Chambers, "Grace monthly ocean mass grids NETCDF release 5.0, ver. 5.0," PO.DAAC, CA, USA, 2012, doi: 10.5067/TEOCN-0N005.

[16] D. P. Chambers and J. A. Bonin, "Evaluation of release-05 GRACE time-variable gravity coefficients over the ocean," *Ocean Sci.*, vol. 8, pp. 859–868, Oct. 2012.

[17] D. P. Chambers and J. K. Willis, "A global evaluation of ocean bottom pressure from GRACE, OMCT, and steric-corrected altimetry," *J. Ocean. Atmos. Technol.*, vol. 27, no. 8, pp. 1395–1402, 2010, doi: 10.1175/2010JTECHO738.1.

[18] D. P. Chambers, B. D. Tapley, and R. H. Stewart, "Long-period ocean heat storage rates and basin-scale heat fluxes from TOPEX," *J. Geophys. Res., Oceans*, vol. 102, no. C5, pp. 10525–10533, 1997.

[19] S. R. Jayne, J. M. Wahr, and F. O. Bryan, "Observing ocean heat content using satellite gravity and altimetry," *J. Geophys. Res., Oceans*, vol. 108, no. C2, p. 3031, 2003, doi: 10.1029/2002JC001619.

[20] (2012). *GHRSST Level 4 CMC0.2deg Global Foundation Sea Surface Temperature Analysis (GDS version 2), ver. 2.0.*, PO.DAAC, CA, USA, doi: 10.5067/GHCMC-4FM02.

[21] B. Brasnett, "The impact of satellite retrievals in a global sea-surface-temperature analysis," *Quart. J. Meteorol. Soc.*, vol. 134, no. 636, pp. 1745–1760, 2008, doi: 10.1002/qj.319.

[22] J. A. Church and J. N. White, "Sea-level rise from the late 19th to the early 21st century," *Surv. Geophys.*, vol. 32, nos. 4–5, pp. 585–602, 2011, doi: 10.1007/s10712-011-9199-1.

[23] A. Cazenave, H. B. Dieng, B. Meyssignac, K. Von Schuckmann, B. Decharme, and E. Berthier, "The rate of sea-level rise," *Nature Climate Change*, vol. 4, no. 5, p. 358, 2014, doi: 10.1038/nclimate2159.

[24] J. T. Reager, A. S. Gardner, J. S. Famiglietti, D. N. Wiese, A. Eicker, and M. H. Lo, "A decade of sea level rise slowed by climate-driven hydrology," *Science*, vol. 351, pp. 699–703, Feb. 2016, doi: 10.1126/science.aad8386.

[25] L. Cheng, K. E. Trenberth, J. Fasullo, T. Boyer, J. Abraham, and J. Zhu, "Improved estimates of ocean heat content from 1960 to 2015," *Sci. Adv.*, vol. 3, no. 3, p. e1601545, 2017, doi: 10.1126/science.aad8386.

[26] B. S. Ferster, B. Subrahmanyam, and A. M. Macdonald, "Confirmation of ENSO-Southern Ocean teleconnections using satellite-derived SST," *Remote Sens.*, vol. 10, no. 2, p. 331, 2018, doi: 10.3390/rs10020331.